Electronic Supplementary Information

Iridium(III) phosphors with bis(diphenylphorothioyl)amide ligand for efficient green and sky-blue OLEDs with EQE nearly 28%

Jing-Cheng Xia[1], Xiao Liang[1], Zhi-Ping Yan[1], Zheng-Guang Wu[1], Yue Zhao[1], You-Xuan Zheng[1,2,*] and Wen-Wei Zhang[1,*]

[1] State Key Laboratory of Coordination Chemistry, Jiangsu Key Laboratory of Advanced Organic Materials, Collaborative Innovation Center of Advanced Microstructures, School of Chemistry and Chemical Engineering, Nanjing University, Nanjing 210093, P. R. China, *Email - yxzheng@nju.edu.cn; wwzhang@nju.edu.cn

[2] Shenzhen Research Institute of Nanjing University, Shenzhen 518057, P. R. China

General information

^{1}H NMR spectra were measured on a Bruker AM 400 spectrometer. The high resolution electrospray ionization mass spectra (HR ESI-MS) were recorded on an Bruker MTQ III q-TOF. TG measurements were carried out on a TG/DSC_STA449F3 analyzer (METTLER). UV-vis absorption and photoluminescence spectra were measured on a Shimadzu UV-2550 and a Hitachi F-4600 spectrophotometer at room temperature, respectively. Cyclic voltammetry measurements were conducted on a chi600e electrochemical workstation using Fc^+/Fc as the internal standard and scan rate of 0.1 V s^{-1}.

X-ray crystallography

X-ray crystallographic measurements of the single crystals were carried out on a Bruker SMART CCD diffractometer (Bruker Daltonic Inc.) using monochromated Mo Kα radiation (λ = 0.71073 Å) at room temperature. Cell parameters were retrieved using SMART software and refined using SAINT program to reduce the highly redundant data sets. Data were collected using a narrow-frame method with scan width of 0.30° in ω and an exposure time of 5 s per frame. Absorption corrections were applied using SADABS supplied by Bruker. The structures were solved by Patterson methods and refined by full-matrix least-squares on F^2 using the program SHELXS-97. The positions of metal atoms and their first coordination spheres were located from direct-

methods E-maps, other non-hydrogen atoms were found in alternating difference Fourier syntheses and least-squares refinement cycles and during the final cycles refined anisotropically. Hydrogen atoms were placed in calculated position and refined as riding atoms with a uniform value of U_{iso}.

OLEDs fabrication and measurement

All OLEDs were fabricated on the pre-patterned ITO-coated glass substrate with a sheet resistance of 15 Ω sq^{-1}. The deposition rate for organic compounds is 1-2 Å s^{-1}. The phosphor and host were co-evaporated from two separate sources. The cathode consisting of LiF/Al was deposited by evaporation of LiF with a deposition rate of 0.1 Å s^{-1} and then by evaporation of Al metal with a rate of 3 Å s^{-1}. The effective area of the emitting diode is 0.1 cm^2. The characteristics of the devices were measured with a computer controlled KEITHLEY 2400 source meter with a calibrated silicon diode in air without device encapsulation. On the basis of the uncorrected PL and EL spectra, the CIE coordinates were calculated using a test program of the spectra scan PR650 spectrophotometer.

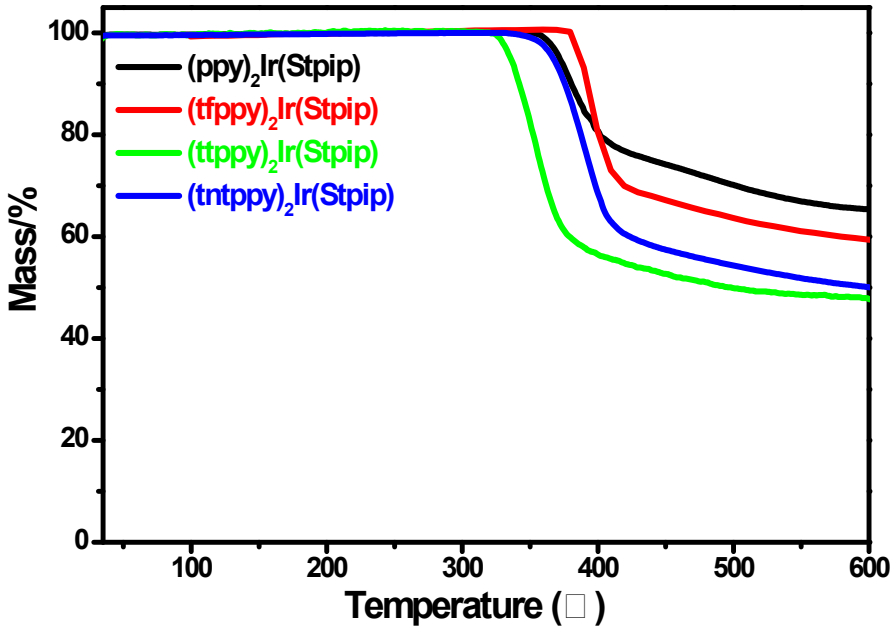

Fig. S1 The TG curves of **$Ir(ppy)_2(Stpip)$**, **$Ir(tfppy)_2(Stpip)$**, **$Ir(ttppy)_2(Stpip)$** and **$Ir(tntppy)_2(Stpip)$**.

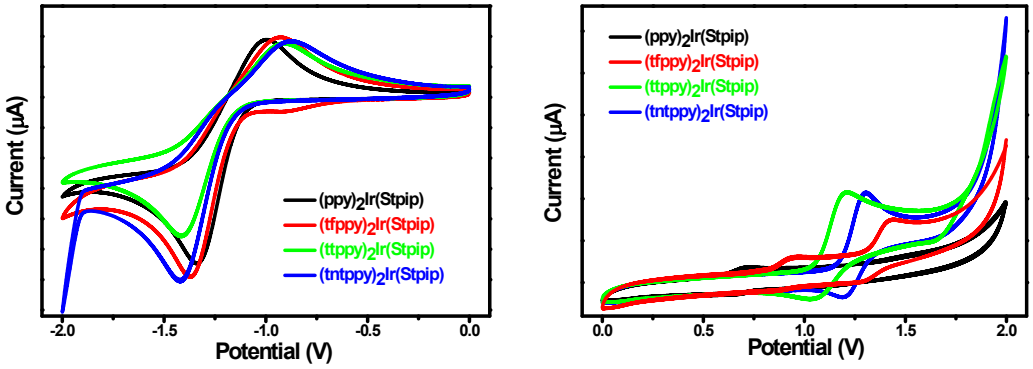

Fig. S2 The cyclic voltammogram curves of **Ir(ppy)$_2$(Stpip)**, **Ir(tfppy)$_2$(Stpip)**, **Ir(ttppy)$_2$(Stpip)** and **Ir(tntppy)$_2$(Stpip)** in degassed CH_2Cl_2 solution at room temperature.

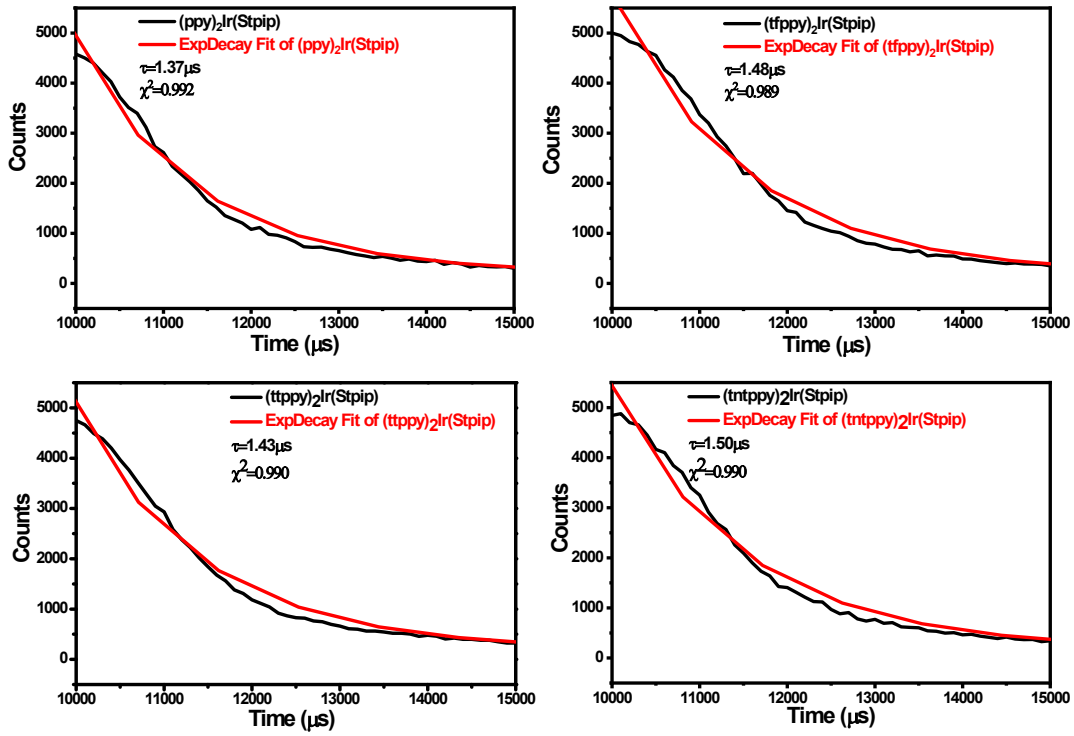

Fig. S3 The lifetime curves of **Ir(ppy)$_2$(Stpip)**, **Ir(tfppy)$_2$(Stpip)**, **Ir(ttppy)$_2$(Stpip)** and **Ir(tntppy)$_2$(Stpip)** in degassed CH_2Cl_2 solution at room temperature.

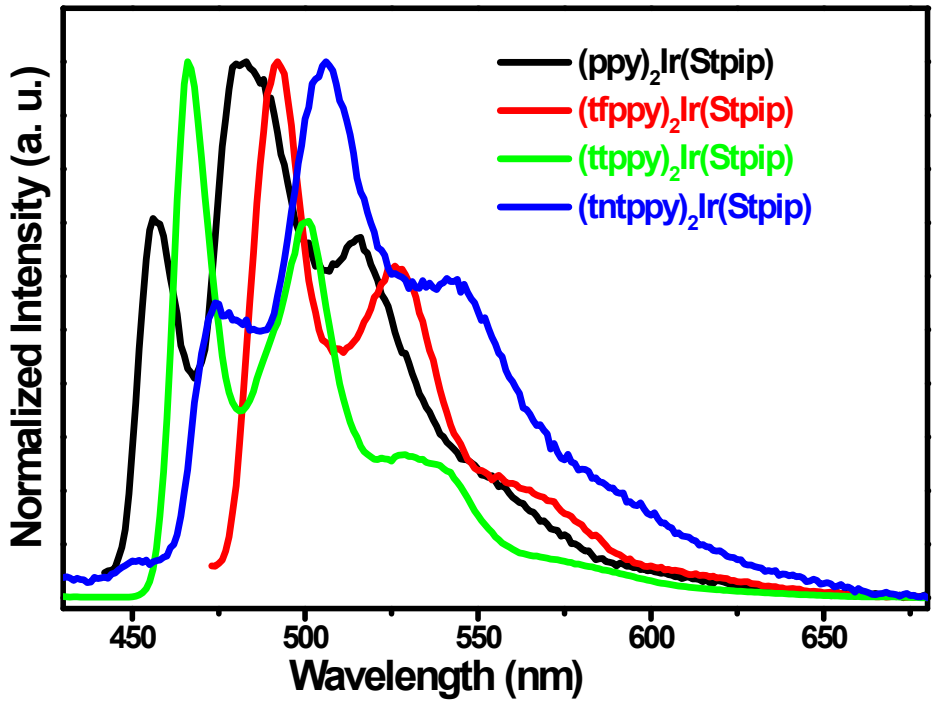

Fig. S4 Emission spectra of **Ir(ppy)$_2$(Stpip)**, **Ir(tfppy)$_2$(Stpip)**, **Ir(ttppy)$_2$(Stpip)** and **Ir(tntppy)$_2$(Stpip)** in degassed CH_2Cl_2 solutions (5×10^{-5} mol L^{-1}) at 77 K.

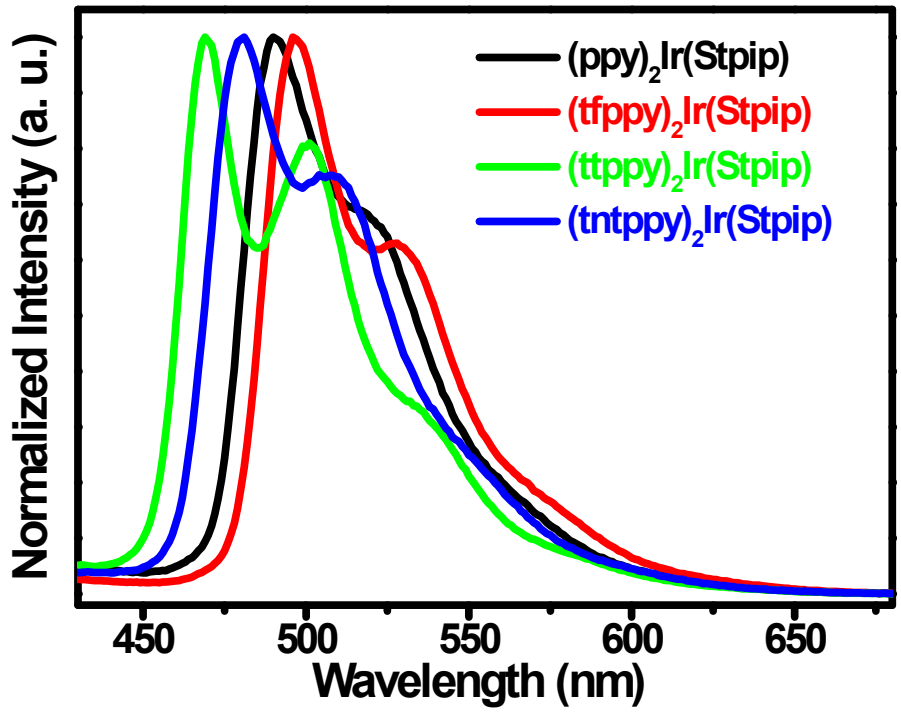

Fig. S5 The PL spectra of **Ir(ppy)$_2$(Stpip)**, **Ir(tfppy)$_2$(Stpip)**, **Ir(ttppy)$_2$(Stpip)** and **Ir(tntppy)$_2$(Stpip)** dopants with the host.

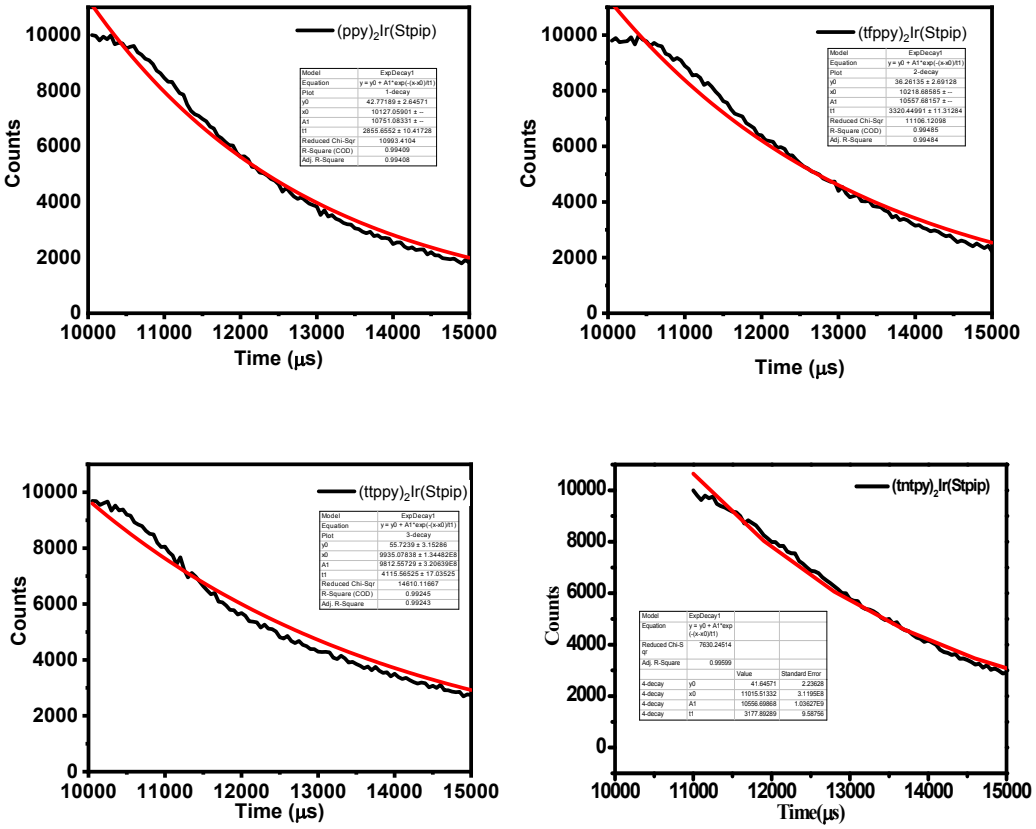

Fig. S6 The lifetime curves of **Ir(ppy)$_2$(Stpip)** (τ = 2.86 μs), **Ir(tfppy)$_2$(Stpip)** (τ = 3.32 μs), **Ir(ttppy)$_2$(Stpip)** (τ = 4.11 μs) and **Ir(tntppy)$_2$(Stpip)** (τ = 3.18 μs) dopant with the host.

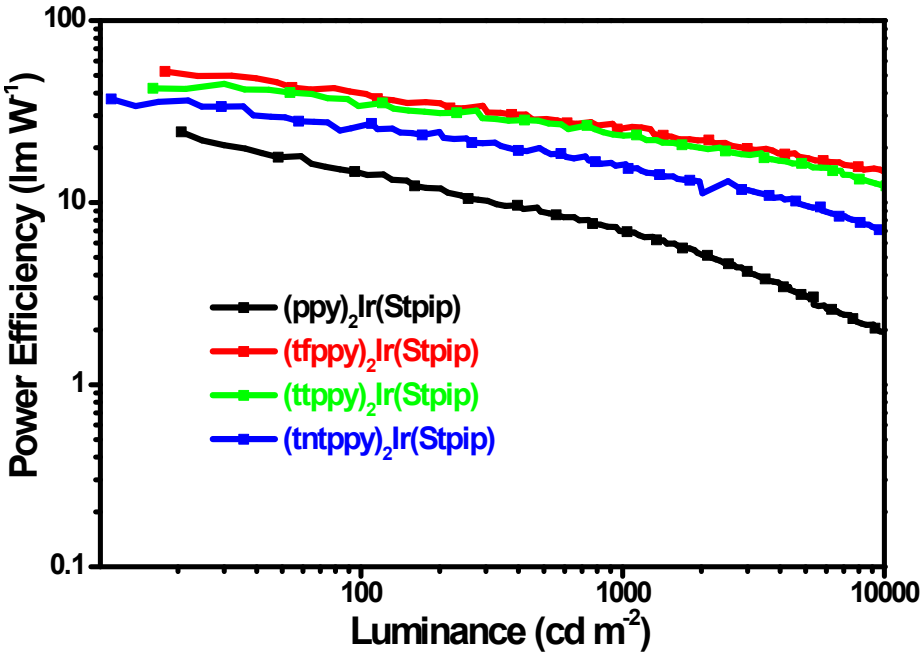

Fig. S7 Power efficiency–luminance (η_p–L) curves of **D1-D4**.

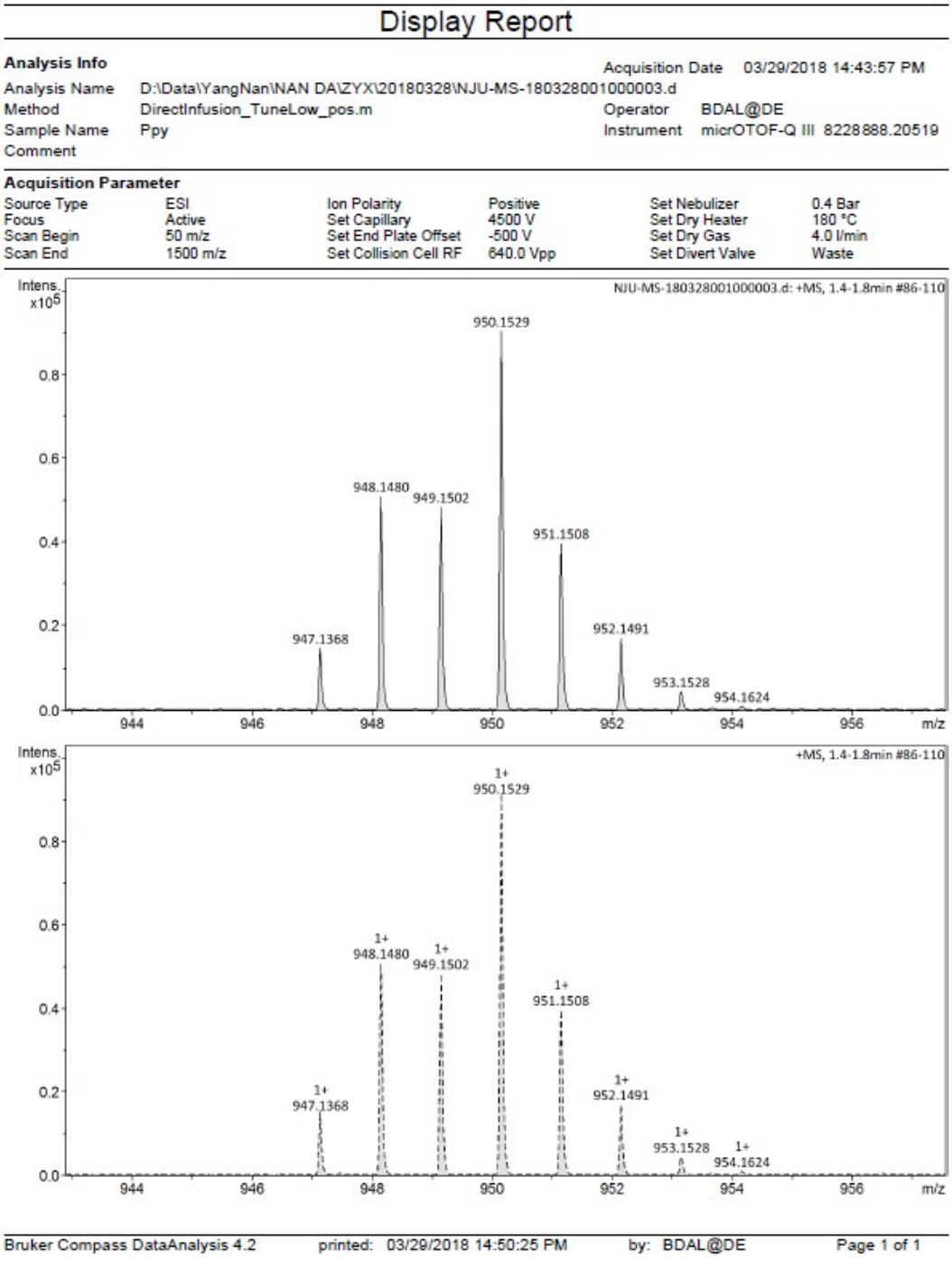

Fig. S8 The mass spectrum of **Ir(ppy)$_2$(Stpip)**.

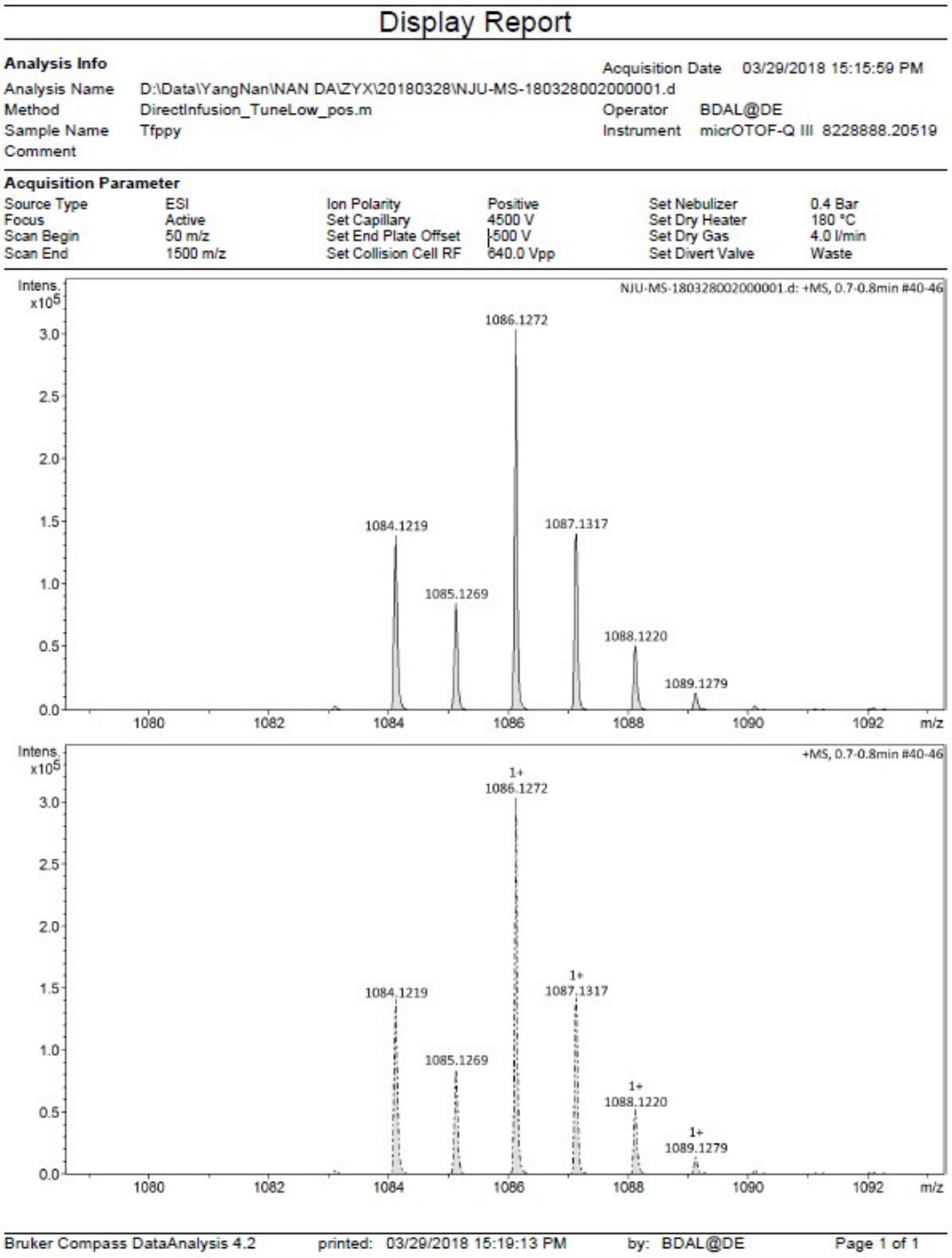

Fig. S9 The mass spectrum of **Ir(tfppy)$_2$(Stpip)**.

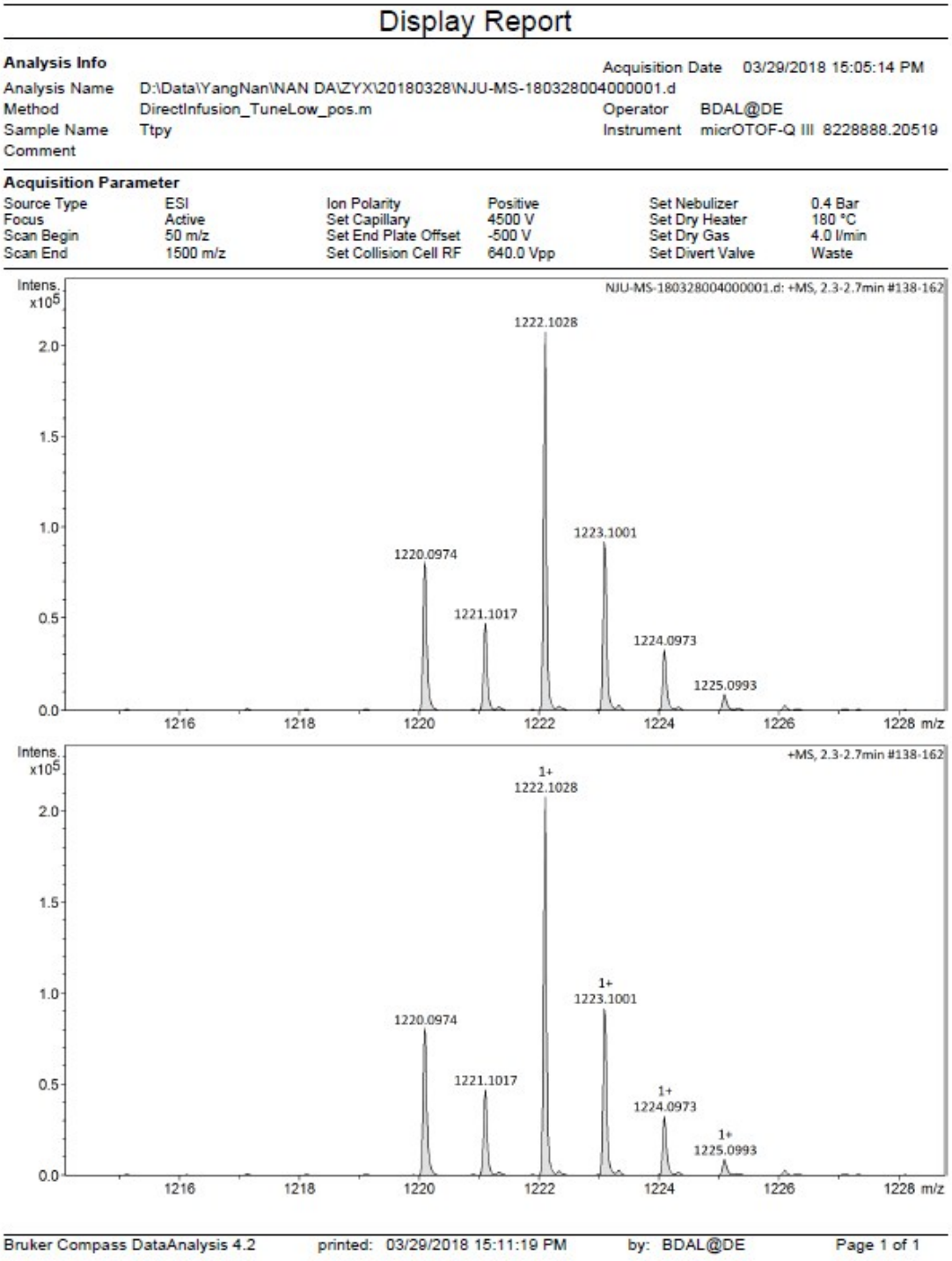

Fig. S10 The mass spectrum of **Ir(ttppy)$_2$(Stpip)**.

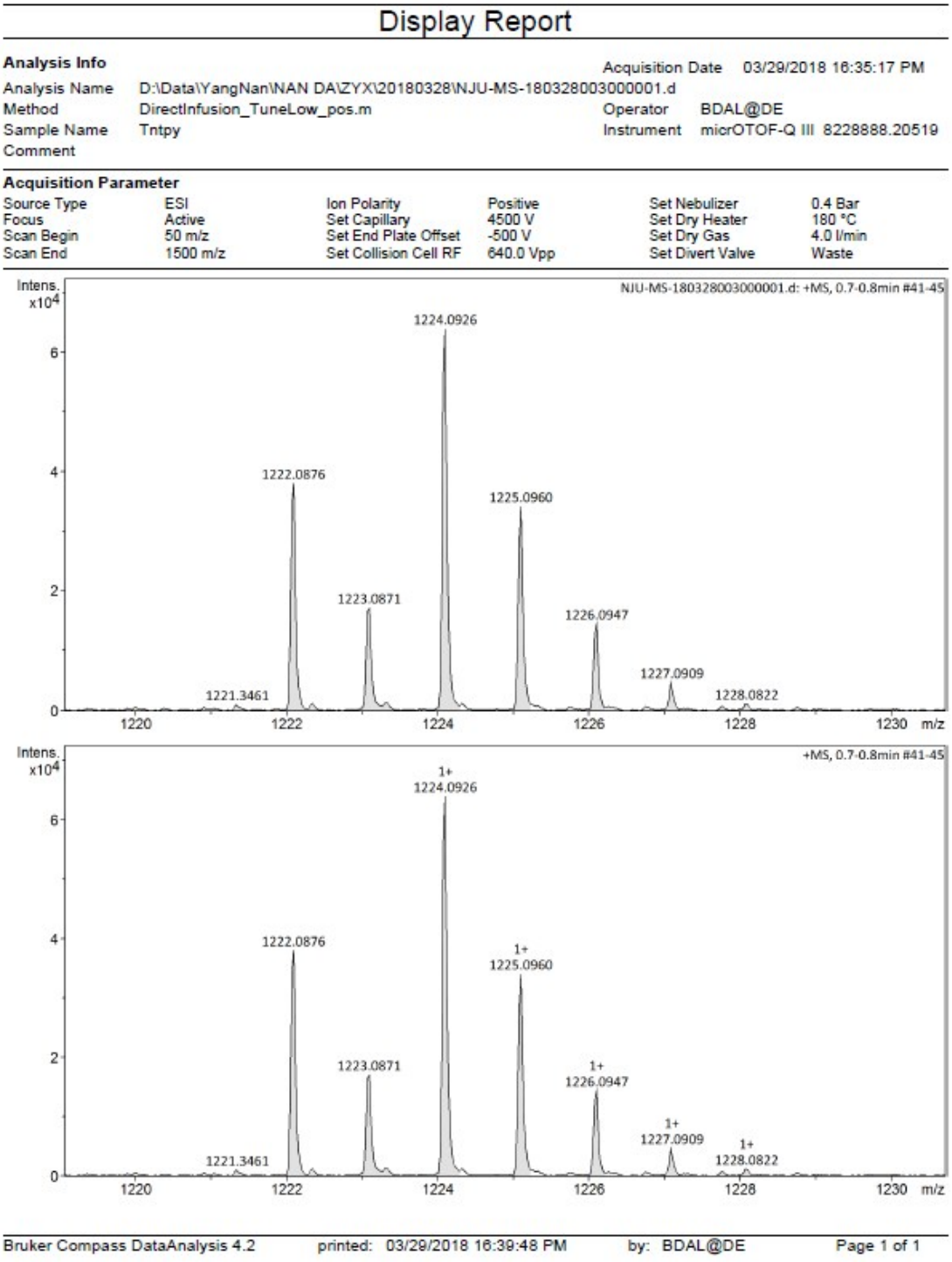

Fig. S11 The mass spectrum of **Ir(tntppy)$_2$(Stpip)**.

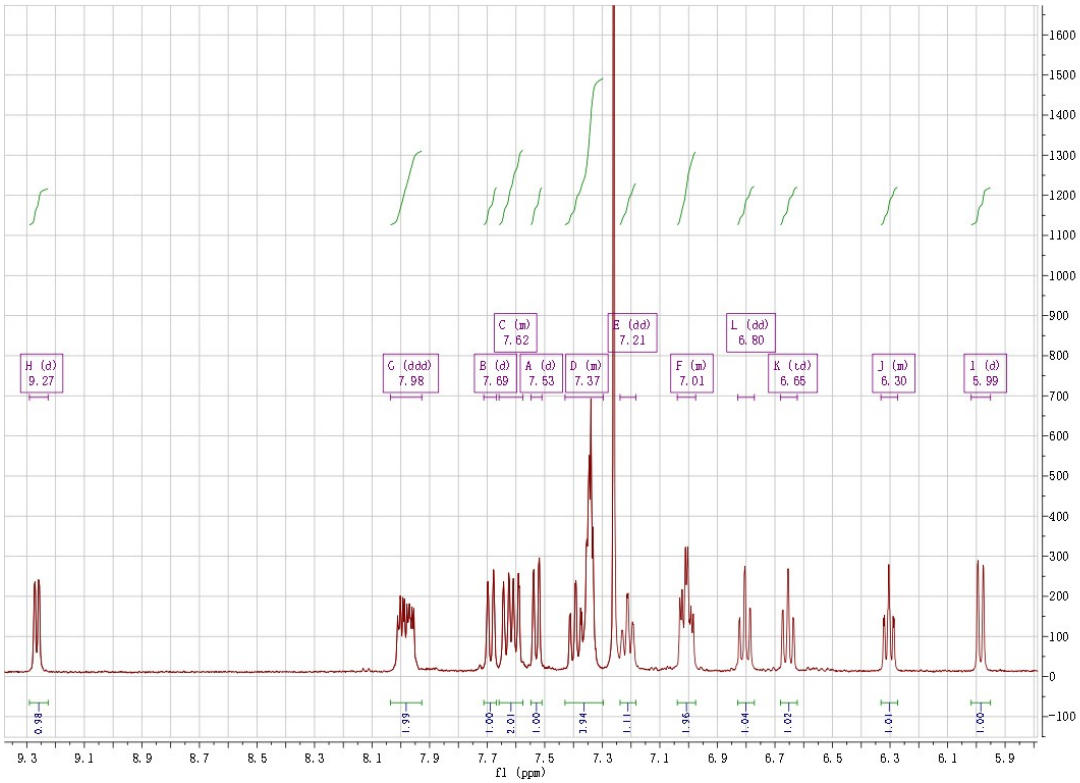

Fig. S12 The ^{1}H NMR spectrum of **Ir(ppy)$_2$(Stpip)**.

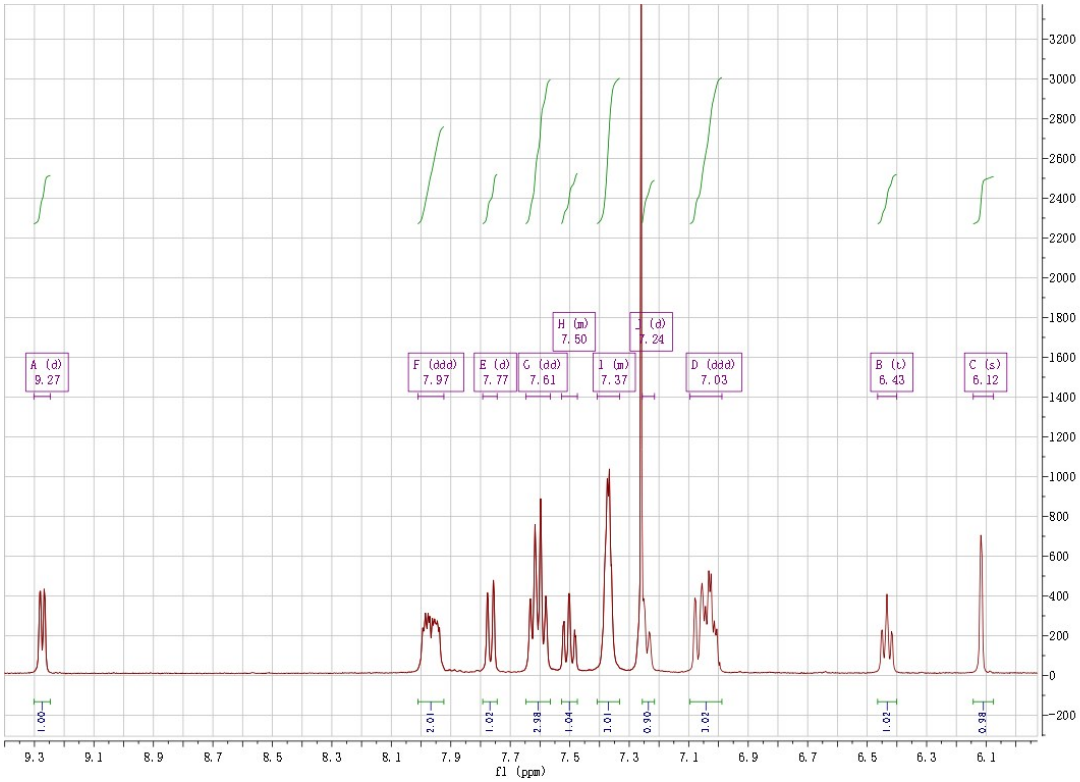

Fig. S13 The ^{1}H NMR spectrum of **Ir(tfppy)$_2$(Stpip)**.

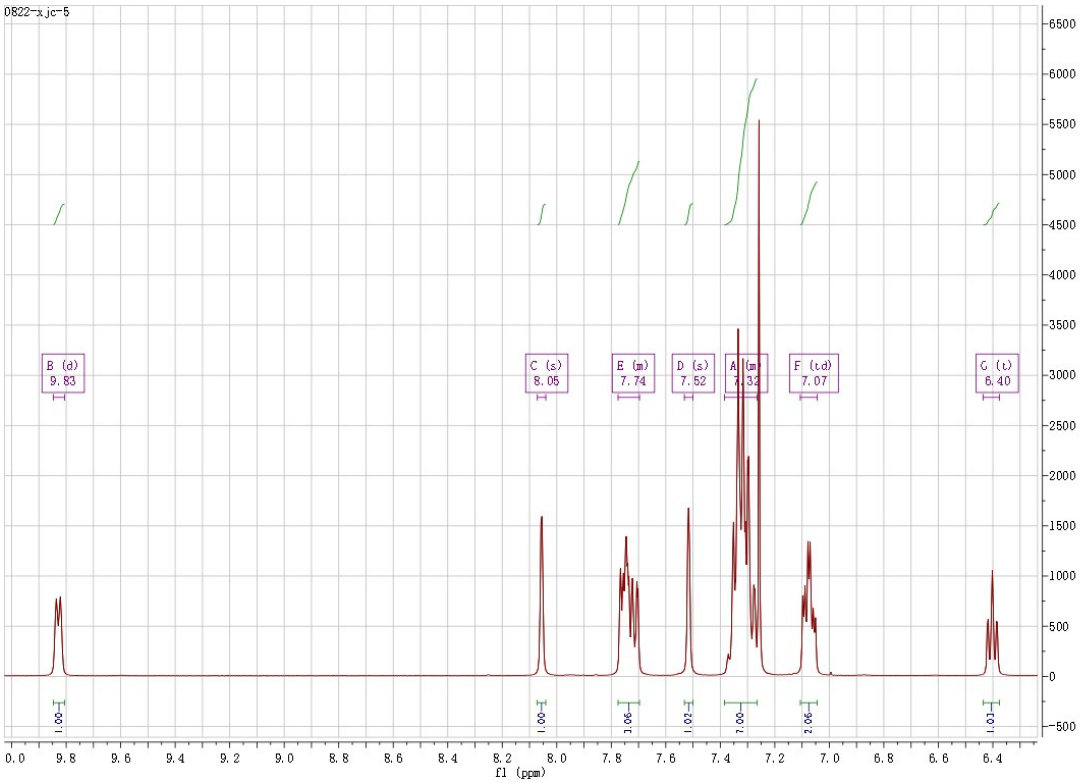

Fig. S14 The ^{1}H NMR spectrum of **Ir(ttppy)$_2$(Stpip)**.

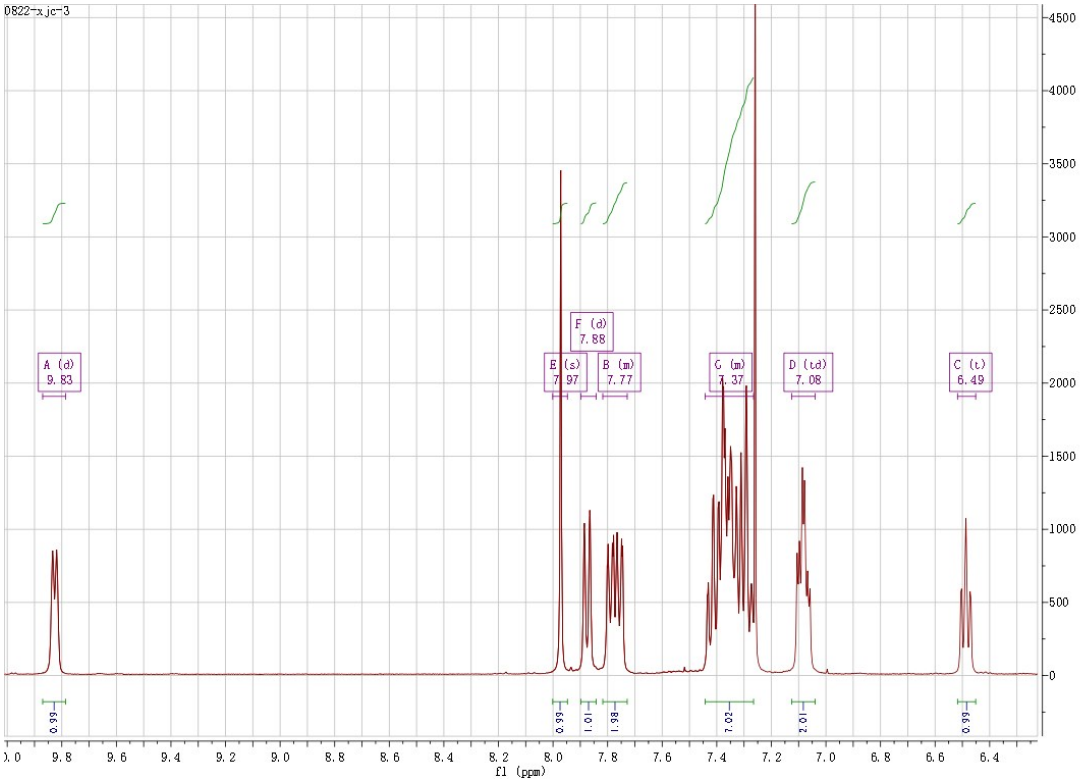

Fig. S15 The ^{1}H NMR spectrum of **Ir(tntppy)$_2$(Stpip)**.

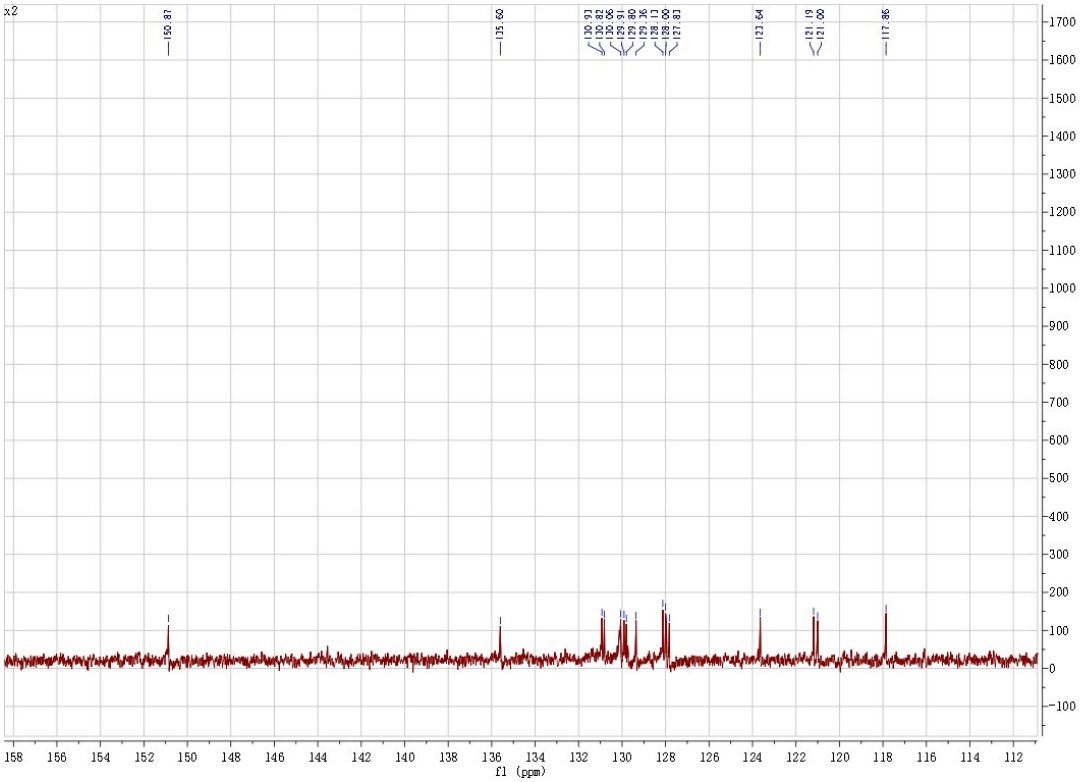

Fig. S16 The ^{13}C NMR spectrum of **Ir(ppy)$_2$(Stpip)**.

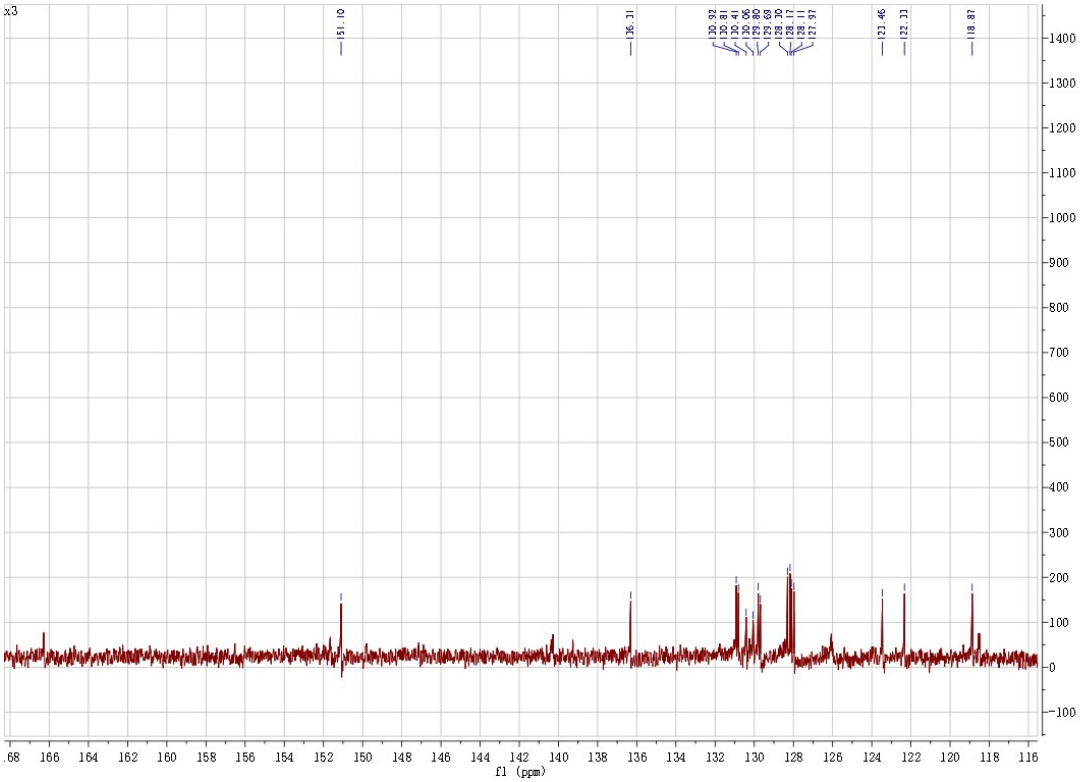

Fig. S17 The ^{13}C NMR spectrum of **Ir(tfppy)$_2$(Stpip)**.

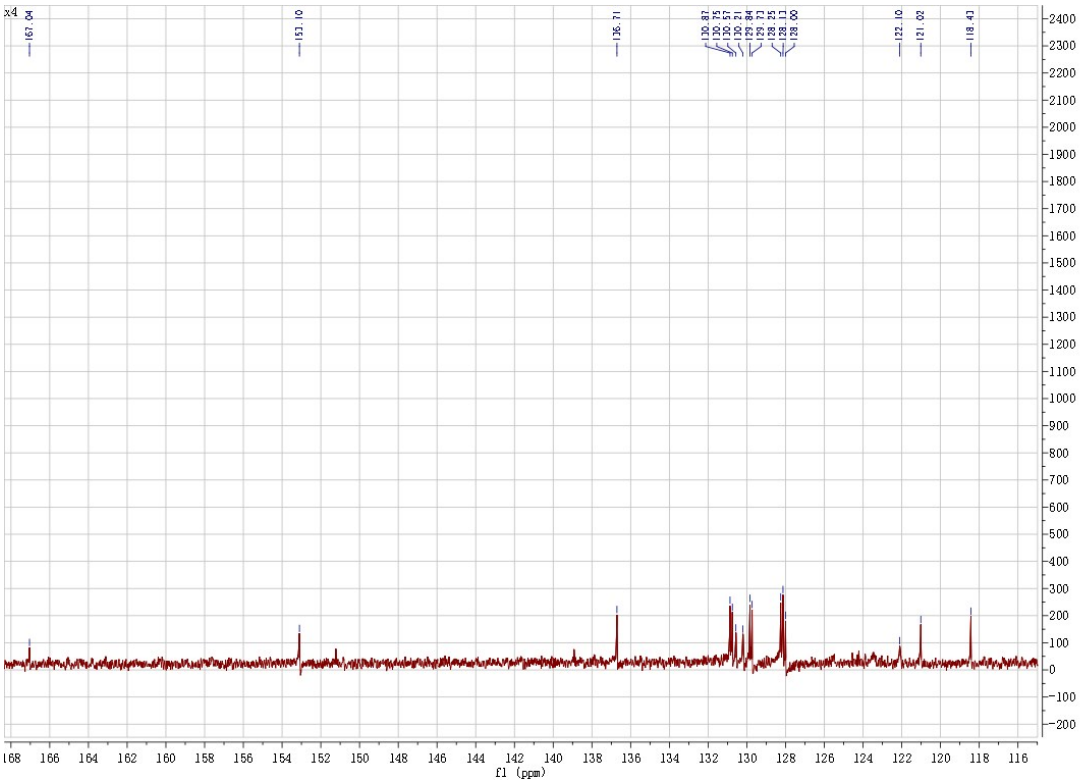

Fig. S18 The ^{13}C NMR spectrum of **Ir(ttppy)$_2$(Stpip)**.

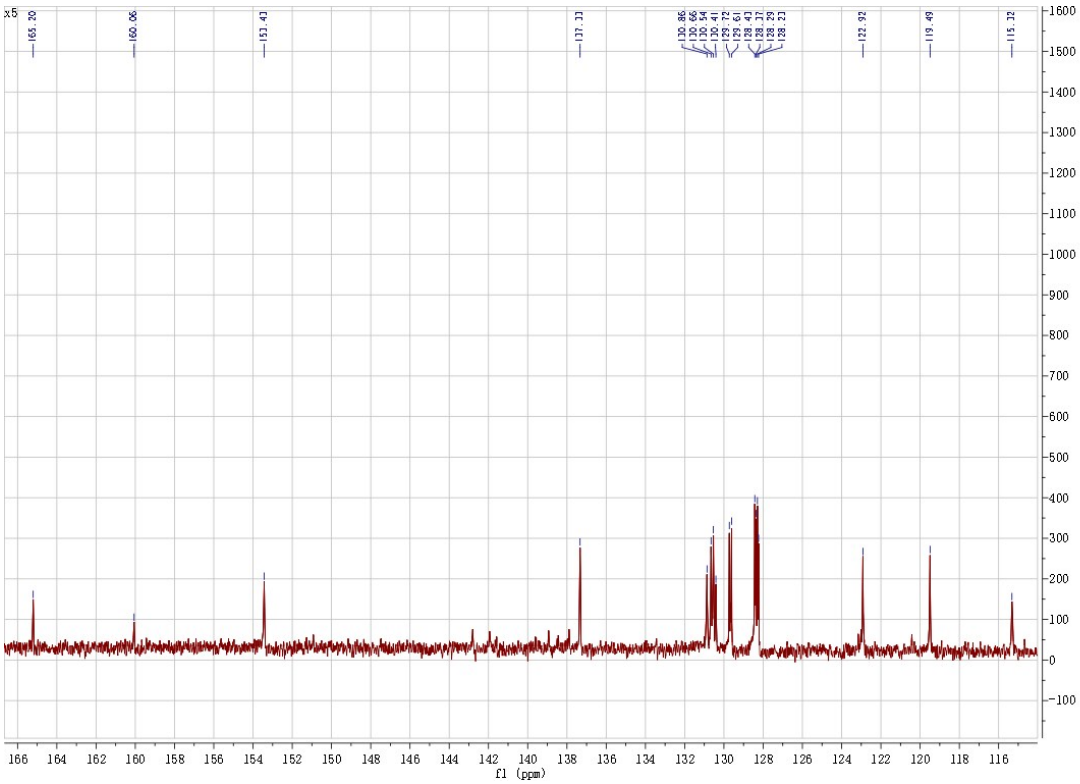

Fig. S19 The ^{13}C NMR spectrum of **Ir(tntppy)$_2$(Stpip)**.

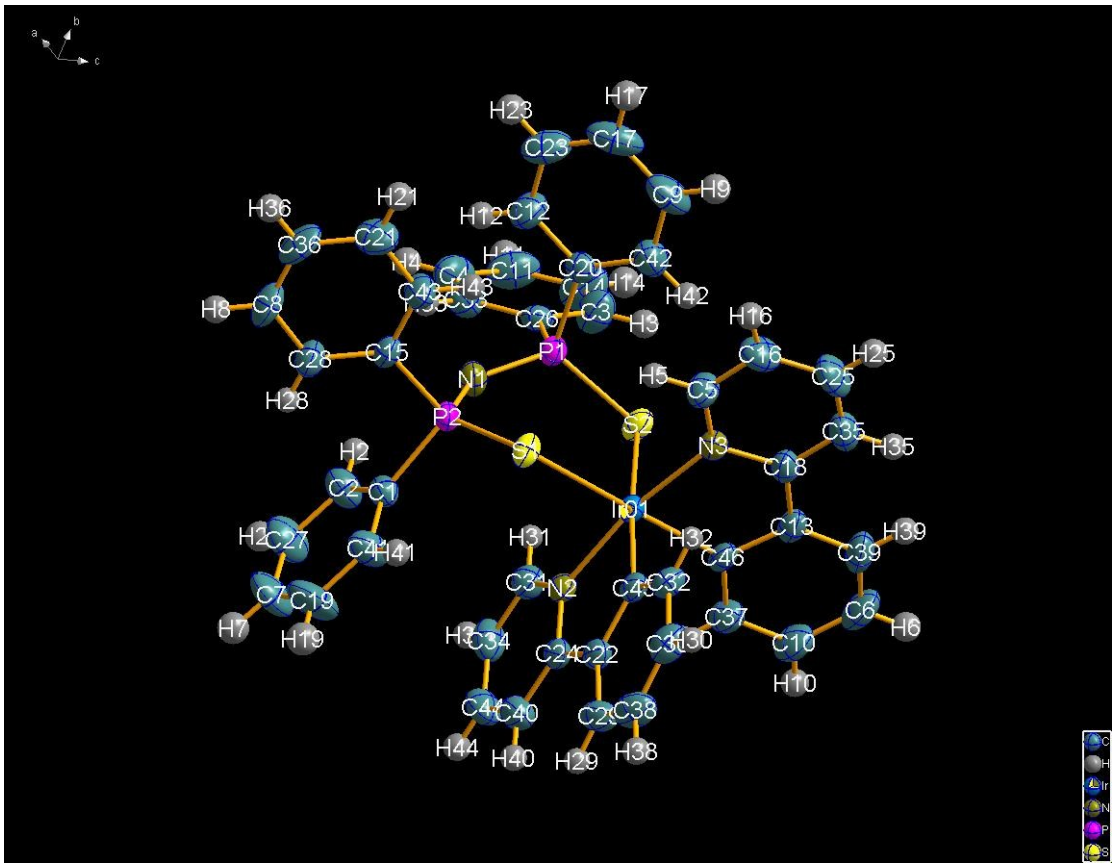

Fig. S20 Single crystal structure of **Ir(ppy)$_2$(Stpip)**.

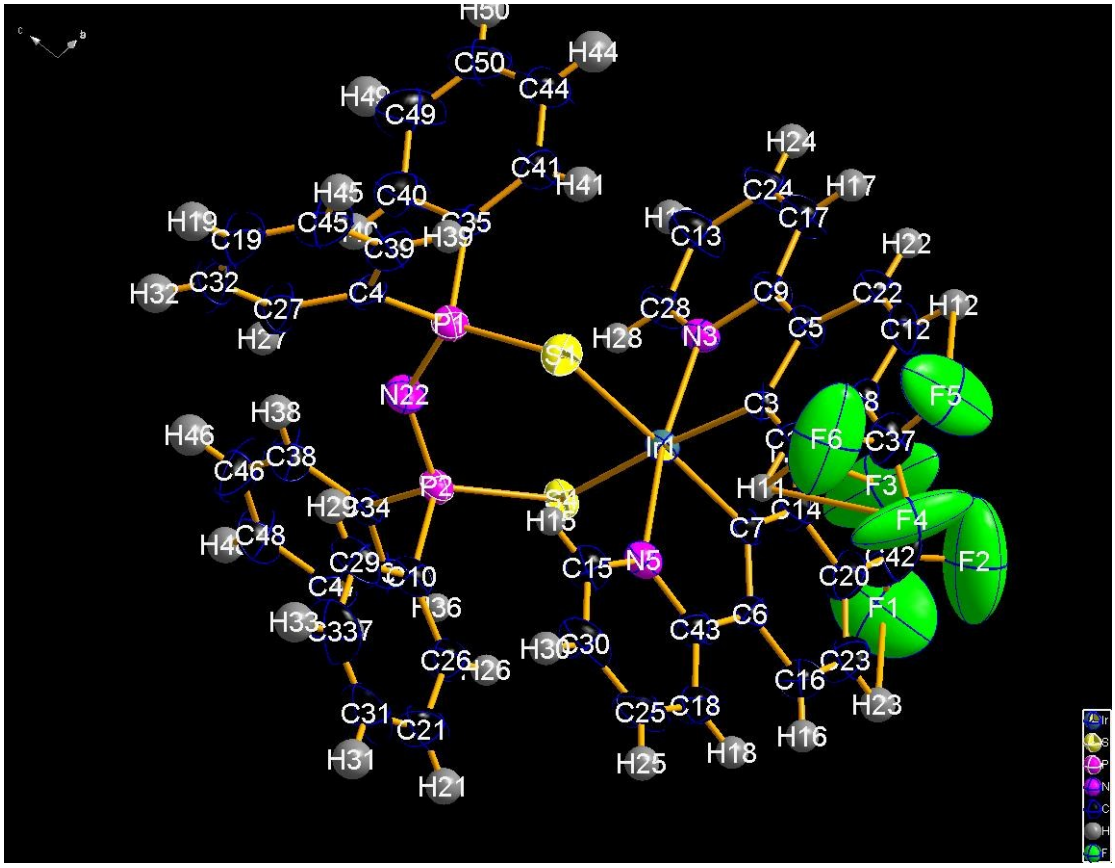

Fig. S21 Single crystal structure of **Ir(tfppy)$_2$(Stpip)**.

Table S1 Crystallographic data of **Ir(ppy)$_2$(Stpip)** and **Ir(tfppy)$_2$(Stpip)**.

	Ir(ppy)$_2$(Stpip)	**Ir(tfppy)$_2$(Stpip)**
Formula	$C_{46}H_{36}IrN_3P_2S_2$	$C_{48}H_{34}F_6IrN_3P_2S_2$
FW	949.04	1085.04
T (K)	296	296
Wavelength (Å)	0.71073	0.71073
Crystal system	Monoclinic	Monoclinic
Space group	P 2 (1) /n	P 2 (1) /c
a (Å)	16.0999(9)	11.6027 (5)
b (Å)	13.7659(8)	16.4388 (7)
c (Å)	17.3693(10)	23.841 (1)
α (deg)	90.00	90
β (deg)	92.617(1)	101.719 (1)
γ (deg)	90.00	90
V (Å^3)	3845.5(4)	4452.5 (3)
Z	4	4
ρ_{calcd} (Mg/m^3)	1.639	1.619
μ (Mo Kα) (mm^{-1})	3.70	3.23
F (000)	1888	2144
Reflns collected	25808	30071
Unique	8811	10180
Data/restraints/params	8811 / 0 / 487	10180/18/559
GOF on F^2	0.901	1.038
R_1[a], wR_2[b] [$I > 2\sigma(I)$]	0.0303, 0.0637	0.0384,0.0860
R_1[a], wR_2[b] (all data)	0.0494, 0.0723	0.0587,0.0940
CCDC NO	1838724	1838723

$R_1{}^a = \Sigma||F_o| - |F_c||/\Sigma|F_o|$. $wR_2{}^b = [\Sigma w(F_o{}^2 - F_c{}^2)^2/\Sigma w(F_o{}^2)]^{1/2}$

Table S2 Selected bond lengths and angels of **Ir(ppy)$_2$(Stpip)** and **Ir(tfppy)$_2$(Stpip)**.

	Ir(ppy)$_2$(Stpip)		**Ir(tfppy)$_2$(Stpip)**
Selected bonds	Bond lengths (Å)	Selected bonds	Bond lengths (Å)
Ir01 C46	2.010(4)	Ir1 C7	2.016(5)
Ir01 C45	2.014(4)	Ir1 C3	2.028(5)
Ir01 N3	2.054(3)	Ir1 N3	2.056(4)
Ir01 N2	2.063(3)	Ir1 N5	2.060(4)
Ir01 S1	2.4883(9)	Ir1 S4	2.4760(12)
Ir01 S2	2.4987(10)	Ir1 S1	2.4923(13)
Selected angels	(^{o})	Selected angels	(^{o})
C46 Ir01 C45	88.32(14)	C7 Ir1 C3	89.98(19)
C46 Ir01 N3	80.61(14)	C7 Ir1 N3	94.14(18)
C45 Ir01 N3	93.22(14)	C3 Ir1 N3	80.31(18)
C46 Ir01 N2	91.64(14)	C7 Ir1 N5	80.26(18)
C45 Ir01 N2	80.25(14)	C3 Ir1 N5	93.40(18)
N3 Ir01 N2	170.05(12)	N3 Ir1 N5	171.64(17)
C46 Ir01 S1	173.41(11)	C7 Ir1 S4	81.71(14)
C45 Ir01 S1	87.05(10)	C3 Ir1 S4	169.56(14)
N3 Ir01 S1	94.96(9)	N3 Ir1 S4	93.92(11)
N2 Ir01 S1	92.20(9)	N5 Ir1 S4	91.43(11)
C46 Ir01 S2	84.53(10)	C7 Ir1 S1	173.28(15)
C45 Ir01 S2	171.97(10)	C3 Ir1 S1	86.72(14)
N3 Ir01 S2	89.21(9)	N3 Ir1 S1	91.07(12)
N2 Ir01 S2	96.29(9)	N5 Ir1 S1	94.08(12)
S1 Ir01 S2	100.37(3)	S4 Ir1 S1	102.17(4)

Table S3 Data of theoretical calculation of orbital energy level and electron cloud distribution

Complex	Orbital	Energy/eV	E_{gap}/eV	Composition (%)		
				Ir	Main ligands	Ancillary ligands
Ir(ppy)$_2$(Stpip)	HOMO	-5.33	3.82	50.13	36.09	13.78
	LUMO	-1.51		4.84	54.31	40.84
Ir(tfppy)$_2$(Stpip)	HOMO	-5.58	3.78	50.12	35.88	13.99
	LUMO	-1.80		3.72	70.85	25.43
Ir(ttppy)$_2$(Stpip)	HOMO	-5.90	4.16	47.76	46.29	5.95
	LUMO	-1.74		4.52	89.13	6.35
Ir(tntppy)$_2$(Stpip)	HOMO	-6.05	3.94	25.77	6.67	67.57
	LUMO	-2.11		3.63	91.33	5.04